Environmental Pollution 283 (2021) 117073

Contents lists available at ScienceDirect

Environmental Pollution

journal homepage: www.elsevier.com/locate/envpol

Disturbed phospholipid metabolism by three polycyclic aromatic hydrocarbons in *Oryza sativa*☆

Shuang Liu [a, b], Na Liu [a, b], Huijie Lu [a], Lizhong Zhu [a, b, *]

[a] College of Environmental and Resource Sciences, Zhejiang University, Hangzhou, Zhejiang, 310058, China
[b] Zhejiang Provincial Key Laboratory of Organic Pollution Process and Control, Hangzhou, Zhejiang, 310058, China

ARTICLE INFO

Article history:
Received 8 February 2021
Received in revised form
28 March 2021
Accepted 31 March 2021
Available online 3 April 2021

Keywords:
Polycyclic aromatic hydrocarbons
Phospholipid
Phospholipase
Phospholipase-coding genes
Oryza sativa

ABSTRACT

Polycyclic aromatic hydrocarbons (PAHs) are ubiquitous pollutants in soils that can be readily absorbed by crops, affecting growth and development. Phospholipids (PLs) are essential components of cell membrane and can indicate cellular responses to various organic pollutants. However, the detailed molecular mechanism of phospholipid metabolism based regulation employed by crops in response to PAHs stresses remains elusive. This study characterized the accumulation patterns of representative PAHs, namely phenanthrene (PHEN), pyrene (PY), and benzo[a]pyrene (BaP) in rice (*Oryza sativa*). Crop's responses to PAHs via the regulation of phospholipid metabolism were also explored. PHEN exhibited the highest accumulation in both roots and shoots, followed by PY and BaP, despite PY exhibited much greater phytotoxicity than the other two PAHs. The exposure to 10–500 μg/L PY resulted in down-regulations of the phospholipase A_2 genes *PLA_2-3*, *PLA_2-4*, and *PLA_2-6* (to 19% of the control without exposure) and phospholipase C genes *PLC-1*, *PLC-2*, and *PLC-4* (to 50% of the control), consistent with the changes in phospholipase activity. The contents of typical PLs, including phosphatidylcholine, phosphatidylethanolamine, phosphatidylglycerol, and phosphatidic acid also decreased to a greater extent than those in the PHEN- and BaP-exposed groups. These were the major reasons for the relatively high phytotoxicity of PY, in terms of growth inhibition and cell membrane damage. These findings provide a more comprehensive understanding of crop responses to PAHs and provide insights into risk assessment of soil PAH contamination, which hold potentials in improving food safety and quality worldwide.

Pyrene inhibited rice growth and reduced cell membrane integrity by affecting phospholipid metabolism to a greater extent than phenanthrene and benzo[a]pyrene.

1. Introduction

Polycyclic aromatic hydrocarbons (PAHs) are a group of ubiquitous organic pollutants in soil environments that originate primarily from incomplete combustion of organic materials such as wood, fossil fuels, and tobacco (Tang et al., 2013). Given their high hydrophobicity, PAHs can be readily adsorbed onto soil particles and become poorly bioavailable (Alexander, 2000). Nevertheless, some PAHs are accumulated in subcellular organelles with high lipid content, such as cell membrane and endoplasmic reticulum, or transformed to more reactive products mediated by enzymes such as cytochrome P450. PAHs accumulation will affect the normal metabolic processes and functions of cells, and can potentially cause irreversible damage to cell membrane integrity (Rajput et al., 2021; Ren et al., 1994). Our previous study showed a close relationship between organic pollutant accumulation and the lipid contents of crops, indicating that lipids may be a major factor influencing the uptake of organic pollutants by crops (Li et al., 2020; Wu and Zhu, 2019). More detailed investigations on lipid synthesis are needed to better understand the uptake, accumulation, and transformation of PAHs in crops.

Phospholipids (PLs) are a major class of lipids in crops; they greatly influence the formation of cell membrane, the composition of intracellular metabolites, and the quality of grains (Liu et al., 2013). However, the levels of PLs in crops are susceptible to various environmental stresses, such as high or low temperature, salts, drought, mechanical wounding, and so on (Hong et al., 2018; Mao et al., 2007; Zhao et al., 2010). Therefore, PLs levels are

☆ This paper has been recommended for acceptance by Baoshan Xing.

* Corresponding author. College of Environmental and Resource Sciences, Zhejiang University, Hangzhou, Zhejiang, 310058, China.
E-mail address: zlz@zju.edu.cn (L. Zhu).

https://doi.org/10.1016/j.envpol.2021.117073
0269-7491/

considered as important indicators of crops' response to environmental stresses. To date, most studies have focused on the impacts of organic pollutants on lipid peroxidation, the structure of the PL membrane bilayer, and membrane permeability. Relatively little information is available regarding the influence of organic pollutants on PLs levels in crops (Vaz Pedroso et al., 2016). In general, the PLs are mainly comprised of phosphatidylcholine (PC), phosphatidylethanolamine (PE), phosphatidylglycerol (PG), and phosphatidic acid (PA) according to the involved hydrophilic heads (e.g., choline, ethanolamine, inositol, and serine) (Choi et al., 2005). Therein, PC is a class of PL that is correlated with the synthesis of the PL membrane (Cowan, 2006). PE produced in endosperm represents the major starch lipid and may form inclusion complexes with amylose, affecting the physicochemical properties and digestibility of starch (Tong et al., 2016). These PLs are involved in the cytidine diphosphate (CDP)-diacylglycerol and 1,2-diacylglycerol (DAG) pathway, and regulated by a series of enzymes, including phospholipase A_2 (PLA_2), phospholipase C (PLC), and phospholipase D (PLD). Among them, PLA_2 mediates the reaction between sn-glycerol triphosphate and acyl-CoA to produce the intermediate product PA. PLC catalyzes the production of DAG from PC, PE, and PG, and PLD catalyzes the transformation of PC and PE to PA (Tong et al., 2016; Zhu et al., 2019). However, comprehensive research on the molecular regulation of PL metabolism in response to organic pollutants is scarce. Previous studies have shown that PAHs are metabolically activated to diol epoxides that can react with DNA, resulting in covalent modifications to the bases or inhibition of gene expressions (Cavallo et al., 2006; Downward et al., 2014; Schinecker et al., 2003). Detailed investigations are needed to reveal the effects of PAHs on the expressions of functional genes involved in PL synthesis and metabolism.

Rice is widely cultivated and consumed worldwide, supplying more than 21% of the global population (Huo et al., 2017; Karlowski et al., 2003). Phenanthrene (PHEN), pyrene (PY), and benzo[a]pyrene (BaP) are among the 16 priority control PAHs specified by the U.S. Environmental Protection Agency (USEPA). Several studies have found that low-ring PAHs are dominant in plants, and their accumulation is related to logK_{ow} (Wu and Zhu, 2019). Therefore, PHEN (tricyclic aromatic hydrocarbons, logK_{ow} = 4.46), PY (tetracyclic aromatic hydrocarbons, logK_{ow} = 4.88) and BaP (pentacyclic aromatic hydrocarbons, logK_{ow} = 6.13) were chosen as the model PAHs for the current exposure experiments. *Oryza sativa* (*O. sativa*) was selected as the model organism to explore the molecular mechanism of its responses to the stresses of these three PAHs, focusing on PL metabolism. The specific objectives were to identify the key PLs and PL metabolic process-involved genes perturbed by the three PAHs, and to elucidate the associations between the expressions of PL metabolic pathways and the physicochemical properties of the three PAHs. A series of 14-day exposure experiments were conducted at varied PAH concentrations. Laser confocal scanning microscope (LCSM) and targeted metabolomics were applied to reveal the morphological and molecular responses, in particular, the effects on PL metabolism of *O. sativa* to the three PAHs. Expected results would enable better risk assessment of PAHs pollution and guide practices to enhance crop yield and quality in PAH polluted soils.

2. Materials and methods

2.1. Chemicals and reagents

Standard stock solutions of phenanthrene (PHEN, CAS No. 85-01-8, purity >99.9%), pyrene (PY, CAS No. 129-00-0, purity >99.9%), benzo[a]pyrene (BaP, CAS No. 50-32-8, purity >99.9%) were purchased from AccuStandard (New Haven, CT, USA). Detailed information for the three chemicals is shown in Table S1. Before the experiment, the stock solution of PHEN, PY, BaP was prepared at 1000 μg/mL in acetone, respectively, and then diluted with deionized water to the concentration of 10, 50, 100, 250, 400, and 500 μg/L as the test solutions. Notably, acetone contents in the test solutions were strictly kept below 0.05% (*v/v*) to minimize the interference of cosolvent (Sun et al., 2013). High-performance liquid chromatography-grade reagents, including methyl tert-butyl ether, acetonitrile, hexane, dichloromethane, and acetone, were obtained from Fisher Scientific (Pittsburgh, PA, USA). The rest of the chemicals and reagents used in this study were of analytical grade. The deionized water (18.2 MΩ) was obtained from an Alpha-Q Ultrapure water system from Millipore (Bedford, MA) and used in all experiments.

2.2. Rice cultivation and PAH exposure experiments

Seeds of *O. sativa* japonica (Lianjing-7) were obtained from the College of Agriculture and Biotechnology, Zhejiang University (Hangzhou, China), because the Lianjing-7 were widely cultivated in the Yangtze River Delta and more tolerant to environmental stress (Chen et al., 2019a). The deflated seeds were removed in flotation. The seeds those plump, unbroken on the surface and similar in size were selected to disinfect by 3% H_2O_2 solution for 30 min, and then soaked in deionized water for 48 h in the dark. After germination, the seeds were incubated in the plant hydroponic boxes contained Hoagland'solution and transplanted into a greenhouse for hydroponics with 25 ± 0.5 °C of temperature and 70 ± 5% of the relative humidity (Hoagland and Arnon, 1950). The temperature and relative humidity were automatically controlled by humidifiers and air conditioning. The detailed components of Hoagland nutrient solution were presented in Supplementary Material Table S2. After grown to 10–12 cm height for 8 days, six seedlings with similar growth were then transferred into a 150 mL brown reagent bottle with a 120 mL test solution. Three parallels were conducted for each concentration of exposure chemicals, including cosolvent control treatments containing deionized water with 0.05% (*v/v*) acetone. The brown reagent bottles were sealed with parafilm to prevent volatilization and were put in the greenhouse with light for 16 h·per day. After exposure for 14 days, the roots and shoots were separated and selected as the objects for downstream analysis, because the roots were directly exposed to the pollutant aqueous solution and the shoots were the major tissue responsible for lipids production.

2.3. Cell membrane integrity assay

For electron microscope analysis, the seeding roots and leaves were cut into 1 mm × 5 mm pieces and fixed by adding 2.5% (*v/v*) glutaraldehyde overnight at 4 °C. After rinsed three times with phosphate buffer (0.1 mol/L, pH7.0), the samples were fixed by 1% osmium acid solution for 1.5 h and then rinsed three times again. Next, the samples were dehydrated with a gradient concentration of ethanol solution (50, 60, 70, 80, 90, 95, and 100%, *v/v*) and transferred to acetone solution for processing. The samples were treated with a mixture of Spurr embedding agent and acetone (1:1, *v/v*) for 1 h and then treated with a mixture of Spurr embedding agent and acetone (3:1, *v/v*) for 3 h. Finally, the samples were treated with a pure embedding agent overnight at room temperature. Thin sections stained with uranyl acetate and lead citrate were examined in a Hitachi H-7650 electron microscope (Bio-ultrastructure analysis Lab, Zhejiang Univ, China) (Liu et al., 2009). The contents of malondialdehyde (MDA) of the roots and shoots were determined based on the methods described previously (Lin et al., 2020). The membrane permeability was analyzed by measuring the

electrical conductivity of cell leakages using a modified technique of Sayyari et al. (2009). The detailed procedure was presented in Supplementary Material Text S1.

2.4. Determination of PAHs by GC–MS

The roots and shoots of seeding were freeze-dried in a vacuum freeze dryer and homogenized by a high-throughput tissue homogenizer (TL-48, Shanghai Onebio Biotech Co., Ltd, China). The roots or shoots (0.1 g) from each sample were weighed accurately and added in 20 mL n-hexane/Methyl *tert*-butyl ether (1:1, *v/v*). After ultrasonicated for 30 min, all samples were centrifuged at 2500 rpm for 5 min and then collected the supernatants. The extraction step was repeated twice for each sample (a total of three extractions). The supernatants from each of the three sequential extractions were combined and dried under N_2. Before the purification of the extract, anhydrous sodium sulfate (Na_2SO_4) and silica gel (100–200 mesh size) was activated in advance. Here, acidified silica gel was prepared by diluting 30 g of concentrated sulfuric acid into 70 g of activated silica. After purification with acidified silica gel eluted with dichloromethane, the collected extract was concentrated under a gentle stream of nitrogen to dryness and redissolved in 200 μL of hexane. The PAH concentrations in the extract were quantified using a gas chromatography coupled with a quadrupole mass spectrometer system (7890 B–5977 B, Agilent Technologies Co., Santa Calra, CA, USA) equipped with an electron ionization (EI) ion source. The extract was separated on a DB-5 MS capillary column (30 m × 0.25 mm i.d. × 0.25 μm film thickness) with helium (99.999%) as the carrier gas at a constant flow rate of 0.8 mL/min in a splitless mode. The oven temperature was initially kept at 80 °C and was increased to 220 °C at a rate of 10 °C/min and then to 300 °C at a rate of 5 °C/min, holding for 5 min. The temperature of the ion source and the quadrupole were 180 °C and 280 °C, respectively (Kang et al., 2010; Pan et al., 2018). Notably, no parent compound was detected in control (CK), confirming no cross-contamination occurred in the growth chamber.

The cross-section of rice roots was analyzed under a Zeiss LSM 880 laser confocal scanning microscope (Zeiss, Germany) with a PlanApochromat 20/0.8 DIC objective lens for three PAHs imaging exposed with 100 and 500 μg/L PHEN, PY, and BaP solution. PHEN, PY, and BaP were imaged by excitation at 405 nm, and the emitted fluorescence was detected at 405–700 nm. The fluorescence intensity was integrated to quantify the PHEN, PY, and BaP contents. The maximum pixel value was never larger than 255, and fluorescence saturation was not detected in any experiment (Wu et al., 2018).

2.5. Phospholipid extraction and quantification by LC–MS/MS

Briefly, rice shoots were ground using ceramic mortar and pestle pre-cooled with liquid nitrogen. Then, 25 mg of the powder was used for phospholipid extraction using 5 mL of methanol: Methyl *tert*-butyl ether: water (1:3:1, *v/v/v*) mixture. After incubation and sonication for 20 min in an ice-cooled sonic bath, each sample was added in 800 μL of water: methanol (3:1, *v/v*). This led to the formation of two phases: a lipophilic phase and a polar phase. The lipophilic phase was collected, vacuum-dried. The dried phospholipid extracts were re-suspended in 500 μL buffer (acetonitrile: isopropanol, 7:3) and transferred to a glass vial (Chen et al., 2019b).

The phospholipid levels in rice shoot were quantified using liquid chromatography coupled with a quadrupole mass spectrometer system (7890 B–5977 B, Agilent Technologies Co., Santa Calra, CA, USA) equipped with an electrospray ion source (ESI). The column used was a reverse phase C18 column (Agilent, USA). The initial mobile phase composition was methanol with 0.1% formic acid (mobile phase A) and isopropanol with 0.1% formic acid (mobile phase B). The gradient separation was performed at a flow rate of 200 μL/min, which set to 3 min 75% A; 5 min linear gradient from 75 to 60% A; 25 min linear gradient from 60 to 35% A; 30 min linear gradient from 35 to 5% A. After washing the column for 33 min with 5% A, the buffer was set back to 75% A, and the column was re-equilibrated for 4 min. The MS was set to positive and negative ion modes, using targeted selected ion monitoring acquisition mode (Bustamant et al., 2017).

2.6. Quantitative real-time PCR (qRT-PCR)

Relative expression was determined by performing qRT-PCR in an iCycler iQ detection system with the Optical System Software version 3.0a (Bio-Rad, Hercules, CA), using the intercalation dye SYBR Green I (Invitrogen, Carlsbad, CA) as a fluorescent reporter, with 2.5 mmol/L $MgCl_2$; 0.5 μmol/L of each primer and 0.04 U/μL of GoTaq Polymerase (Promega, Madison, WI). PCR primers were designed based on rice cDNA sequences published in China Rice Date Center (http://www.ricedata.cn/gene) and Phytozome (https://phytozome.jgi.doe.gov), using NCBI Database (https://www.ncbi.nlm.nih.gov/tools/primer-blast) (www.frodo.wi.mit.

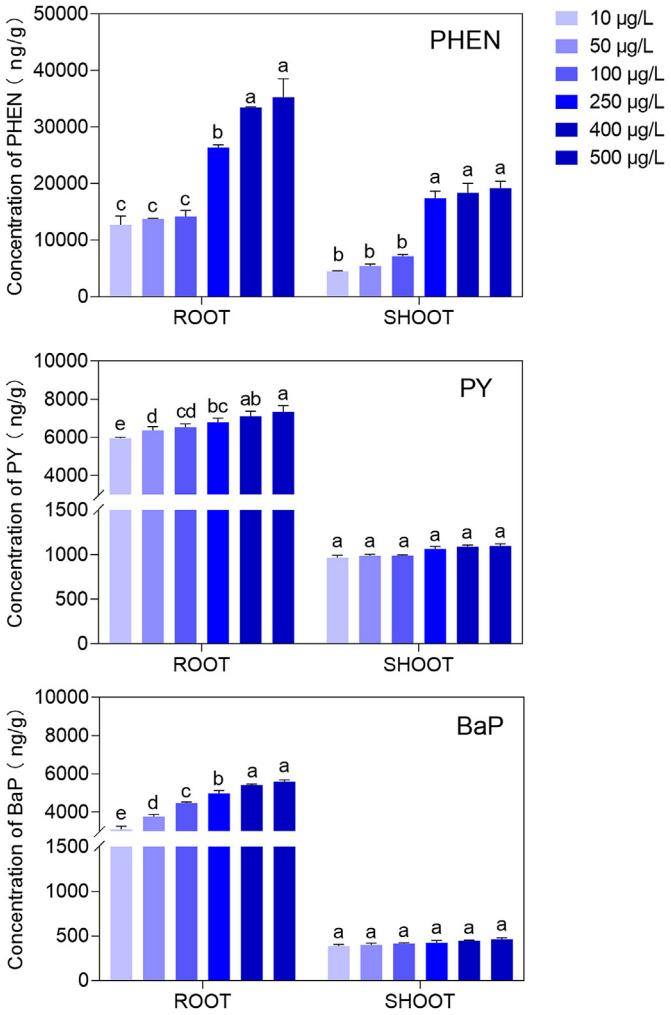

Fig. 1. Accumulations of phenanthrene (PHEN), pyrene (PY) and benzo[a]pyrene (BaP) in rice roots and shoots at different exposure levels. Error bars represent the standard deviations from triplicate samples. Letters above the bars represent significant differences between groups ($p < 0.05$).

edu/cgibin/primer3/primer3) in order to produce amplicons of 134–230 bp in size. The sequences of primers are listed in Supplementary Material Table S3. A 2-fold dilution of cDNA obtained as described above was used as a template. PCR controls were performed in the absence of added reverse transcriptase to ensure that RNA samples were free of DNA contamination. Cycling parameters were as follows: initial denaturation at 95 °C for 15 min; 40 cycles of 95 °C for 10 s, 55 °C for 20 s and 72 °C for 30 s; and 72 °C for 10 min. Melting curves for each PCR were determined by measuring the decrease of fluorescence with increasing temperature (from 65 to 98 °C). The specificity of the PCRs was confirmed by melting curve analysis. Relative gene expression was calculated using the 'Comparative $2^{-\Delta\Delta CT}$' method and Tubulin as a reference gene. Each RNA sample was run in triplicate and repeated at least with two independent sets of treatments (Livak and Schmittgen, 2002).

2.7. PLA_2, PLC and PLD enzyme assay

Fresh rice shoots were ground to powder with liquid nitrogen.

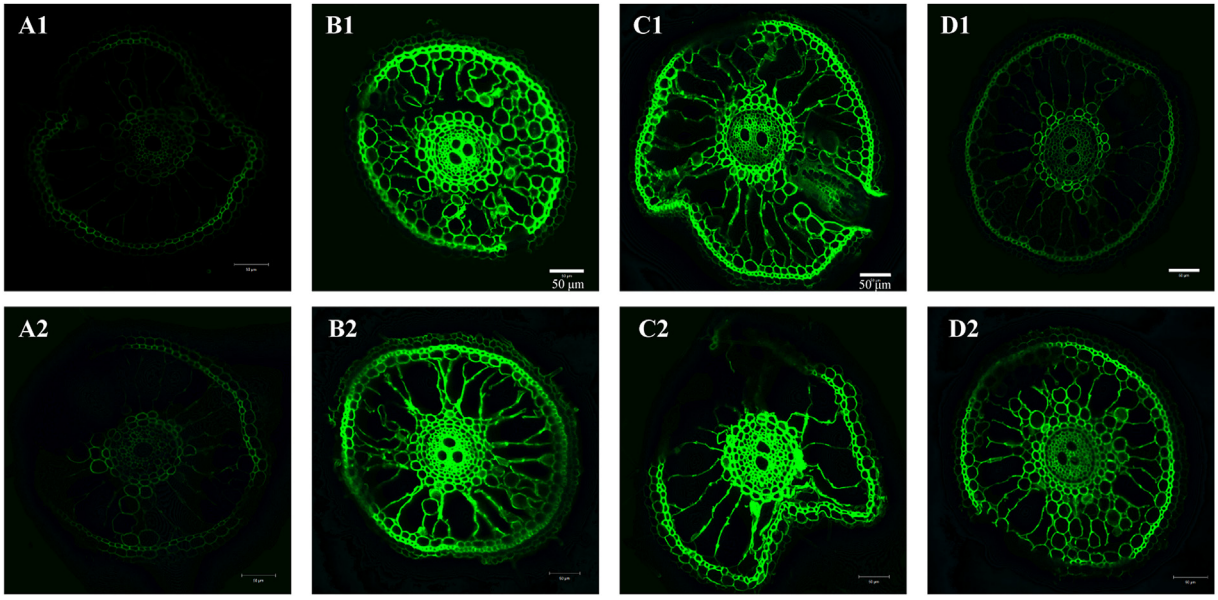

Fig. 2. LCSM micrographs of three PAHs accumulated in the interstitial space of rice root cells. A1 and A2: control groups without PAH exposure; B1: 100 μg/L PHEN; B2: 500 μg/L PHEN; C1: 100 μg/L PY; C2: 500 μg/L PY; D1: 100 μg/L BaP; D2: 500 μg/L BaP.

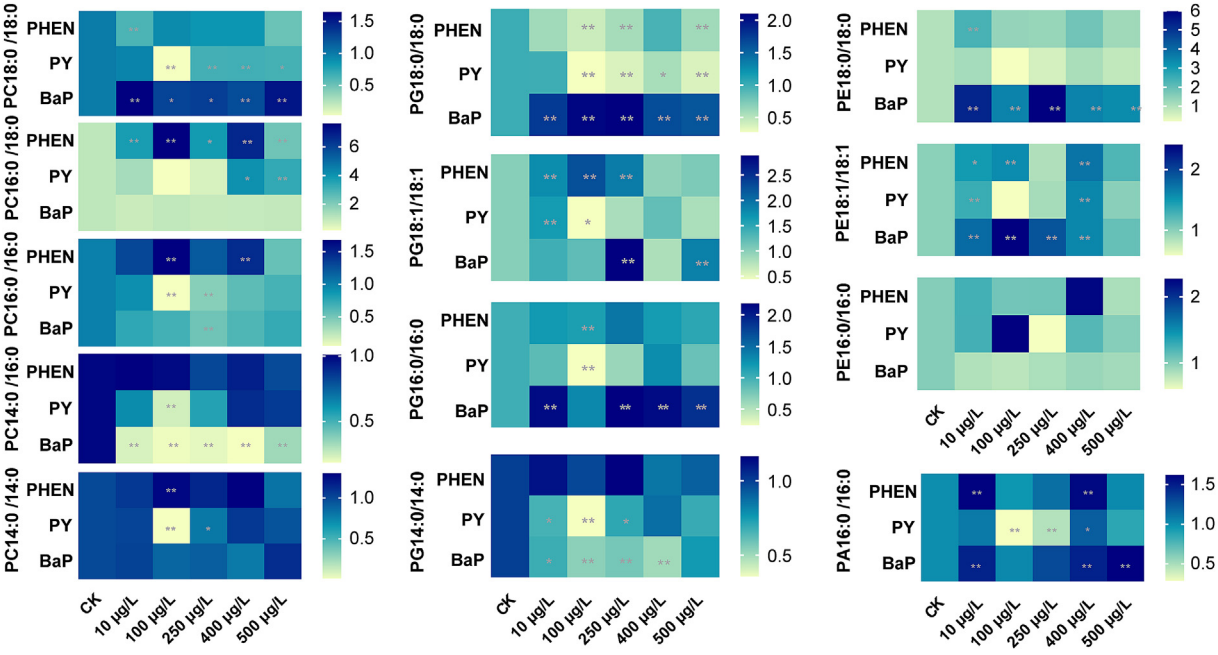

Fig. 3. Heatmaps of phospholipids accumulated in rice shoots after being exposed to different concentrations of PHEN, PY and BaP. The yellow and blue color bars denote low to high contents of phospholipids. PC, phosphatidylcholine; PE, phosphatidylethanolamine; PG, phosphatidylglycerol; PA, phosphatidic acid. Asterisks * and ** represent significance levels at 0.05 and 0.01 based on two-way ANOVA analysis, respectively. (For interpretation of the references to color in this figure legend, the reader is referred to the Web version of this article.)

0.1 g powder was mixed with 0.9 mL of PBS buffer (0.1 mol/L, pH 7.4). After centrifugation at 3000*g* at 4 °C for 15 min, the supernatant was collected for analysis using plant phospholipase A_2 (PLA_2) enzyme-linked immunosorbent assay (ELISA) kit, plant phospholipase C (PLC) enzyme-linked immunosorbent assay (ELISA) kit and phospholipase D (PLD) enzyme-linked immunosorbent assay (ELISA) kit (Meimian Biotechnology Co. Ltd, China).

2.8. Statistical analysis

All samples were performed in three replications. The data were expressed as means ± standard deviation (SD). Statistical analysis was done with GraphPad Prism statistical analysis software (version 8.0, San Diego, CA). Duncan's new Multiple Range Test (DMRT) was used to compare the differences of each treated group. Points denoted by different lower case letters on each bar differ significantly at $p < 0.05$ and at $p < 0.01$, respectively.

3. Results and discussions

3.1. Biomass production stressed by PHEN, PY and BaP

As shown in the Supplementary Material Figs. S1 and S2, PHEN, PY, and BaP significantly inhibited the growth of rice roots and shoots. Overall, as the concentrations of PHEN, PY and BaP increased from 10 μg/L to 500 μg/L, the root biomass decreased by 13.7–28.3%, 51.5–56.5%, and 14.1–27.2%, respectively, compared with those in the control groups without PAHs. Meanwhile, the shoot biomass decreased by 10.3–21.9%, 19.3–24.7%, and 4.03–18.2%, respectively. This suggests that PAHs inhibited rice growth in a dose-dependent manner. Similar results have been observed in *Alternanthera Philoxeroides*, where the growth of roots and shoots was inhibited by PHEN and PY at different levels depending on their doses. Further, PY reduced *A. philoxeroides* growth more than PHEN (Huang et al., 2019). In the current study, the biomass of the roots and shoots in the PY-exposed groups was significantly lower than that in the PHEN- and BaP-exposed groups, consistent with the results from the above study on the toxicity of PHEN and PY to *A. philoxeroides*. However, this finding is contrary to that of Ahammed et al. (2012) who found that PHE was more toxic to tomatoes than PY. Sverdrup et al. (2003) compared the phytotoxicity of four PAHs, including PHEN, PY, fluoranthene, and fluorene. The results indicated that growth inhibitions varied for different species and exposure levels. Nevertheless, there have been no detailed studies regarding the effects of PAHs on rice at the cellular and molecular levels.

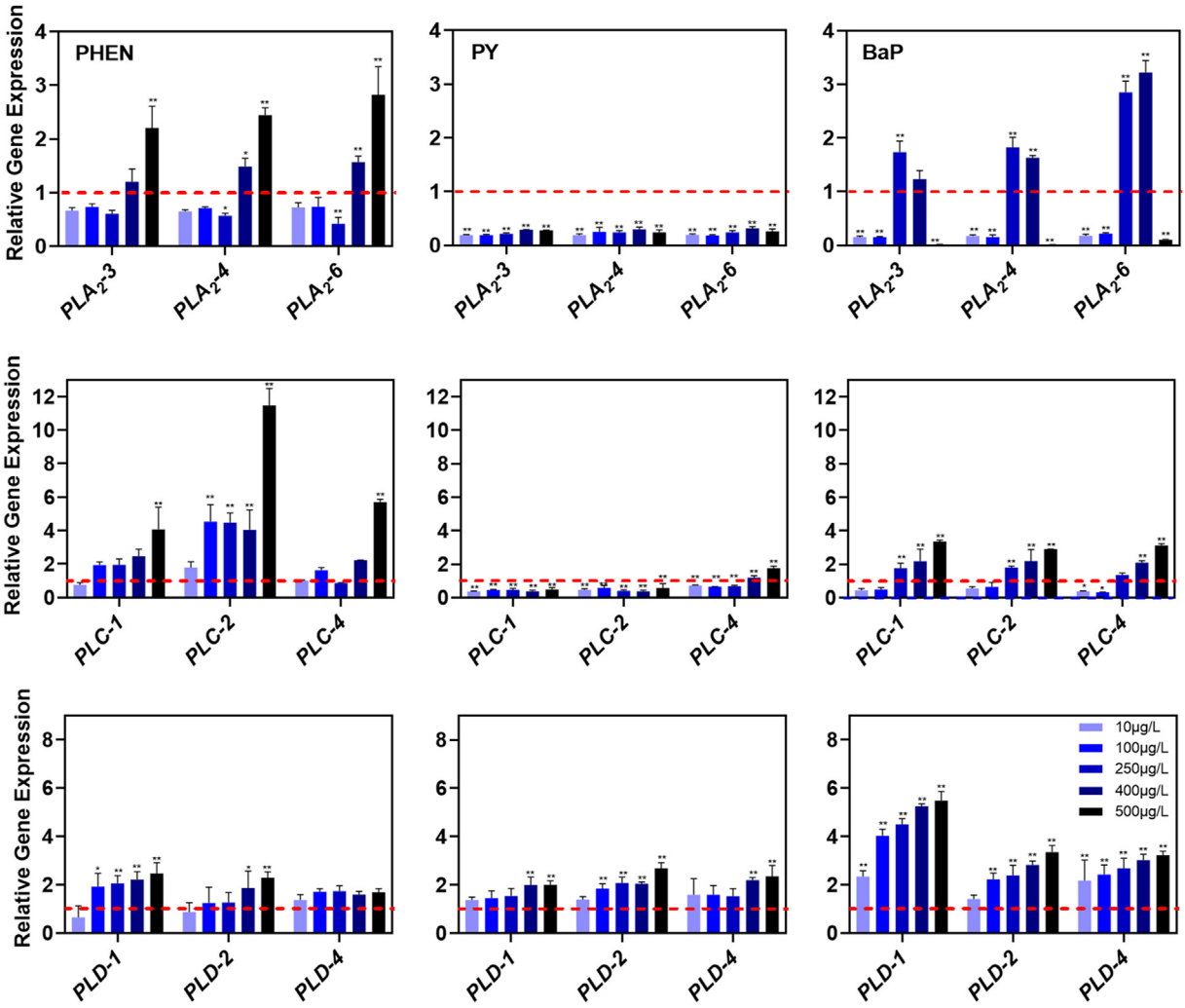

Fig. 4. Expressions of phospholipase encoding genes after being exposed to different concentrations of PHEN, PY and BaP. Gene relative expression levels were the fold changes in PAHs-exposed groups relative to the control groups. *$p < 0.05$; **$p < 0.01$.

3.2. Accumulations of PAHs and cell membrane damage in roots and shoots

The contents of PHEN, PY, and BaP in rice roots and shoots were measured at varying exposure levels. Each PAH content in the roots was 1.8- to 12.0-fold higher than that of the shoots, suggesting that PAH was indeed transported from the roots to the leaves (Fig. 1). Moreover, PHEN accumulation in both the roots and shoots was much higher than that of PY and BaP, which may be attributed to its relatively low logK_{ow} (BaP (6.13) > PY (4.88) > PHEN (4.46)) (EPA, 2016). Sushkova et al. (2020a) reported the maximum accumulation of PHEN among the 16 priority PAHs in most of the soil and plant samples. Generally, hydrophobic compounds can strongly bind to the root surface, making them difficult to be transported inside crops, whereas hydrophilic compounds are more accessible in the shoots via the transpiration stream (Burken and Schnoor, 1997). In another study, the accumulation rates of PAHs in *Echinacea purpurea* roots were inversely correlated with logK_{ow} (Pretorius et al., 2018). Additionally, the higher accumulation of PHEN compared to the other two PAHs could also be attributed to their lower molecular weights and steric hindrance. Interestingly, the accumulation of the three PAHs in the roots eventually reached a plateau at an exposure of 400 μg/L (Fig. 1). The maximum accumulation of PHEN, PY, and BaP in shoots otherwise occurred at exposure levels of 250, 10, and 10 μg/L, respectively. The less efficient transport of PY and BaP inside the crop than PHEN was due to their higher logK_{ow} values, larger molecules, and higher steric hindrance (Burken and Schnoor, 1997).

LCSM was used to determine the accumulation of PAHs in rice roots after exposure to 100 and 500 μg/L of each PAH (Fig. 2). The fluorescence intensities were PHEN > PY > BaP, consistent with their measured contents in the roots. Existing evidence indicates that PAHs can be adsorbed on the root cell walls, and their transport efficiencies into the root cells are inversely proportional to their lipophilicity (Kang et al., 2010; Pretorius et al., 2018). BaP, with greater lipophilicity, concentrates in the subcellular walls and interstitial space, which makes it difficult to get into the cell (Wu et al., 2018).

The MDA contents in roots increased by 166%, 268%, and 135% relative to the controls when the rice was exposed to 500 μg/L of PHEN, PY, and BaP, respectively (Fig. S3). Meanwhile, the permeability of cell membranes increased by 63.0%, 111%, and 50.3%, respectively (Fig. S4). There was a similar trend in the rice shoots after exposure to the three PAHs. These results demonstrate that rice shoots and roots suffered the most severe membrane damage during PY exposure. The toxic effects of PAHs were also observed at the intracellular level in the root cells. As shown in Fig. S5, the cell membrane was irregularly thickened upon exposure to PHEN and BaP, while PY induced apparent damage to the cell membrane. This suggests that the root cells resisted PHEN and BaP at 100 and 500 μg/L, but were prone to PY even at 100 μg/L.

3.3. Targeted phospholipid changes in response to PHEN, PY and BaP

Total and individual PLs, including PC, PA, PG, and PE in the control groups and PAH-treated groups, were determined (Fig. S6 and Fig. 3). Total PLs in the shoots increased in the groups exposed to PHEN and BaP compared with the control groups. As PC and PE are the primary constituents in the cell membrane, their accumulation could be beneficial, allowing the rice to relieve the PAH-triggered membrane damage. As displayed in the TEM images, the thickened cell membrane and aggregated granules in the PHEN- and BaP-treated tissues are direct evidence supporting this. In a previous study, two genes (pah1 and pah2) regulated PL synthesis in *Arabidopsis thaliana* (Kroon, 2011). Leaves of the pah1 and pah2 double mutants contained 80% more PLs than the wild type, and exhibited gross changes in endoplasmic reticulum (ER) morphology, indicating massive membrane overexpansion (Craddock et al., 2015). The current results suggest that PHEN and BaP strongly affected PC and PE, respectively. Moreover, a statistically significant increase in PC (16:0/18:0) contents was found in the shoots after exposure to PHEN ($p < 0.05$). Upon exposure to 100 μg/L PHEN, PC (16:0/18:0) accumulated 650% more than that observed in the controls (Fig. 3). Similarly, PE (18:0/18:0) content was 579% higher after exposure to 250 μg/L BaP compared to the controls.

PL contents in shoots showed an overall decreasing trend upon exposure to PY at 100 μg/L, where PC, PG, PE, and PA decreased by 89.1%, 78.3%, 67.9%, and 74.7%, respectively, compared with the control. Moreover, the individual contents of PC (18:0/18:0), PG (18:0/18:0), PE (18:0/18:0) and PA (16:0/16:0) also decreased significantly by 98.0%, 75.3%, 78.8%, and 74.7%, respectively. These results are consistent with the MDA content and permeability of the cell membrane, suggesting that PY-induced membrane damage was more severe than that induced by the other two PAHs. Previous studies showed that high concentrations of PAHs led to significantly increased MDA production, which resulted in damages to

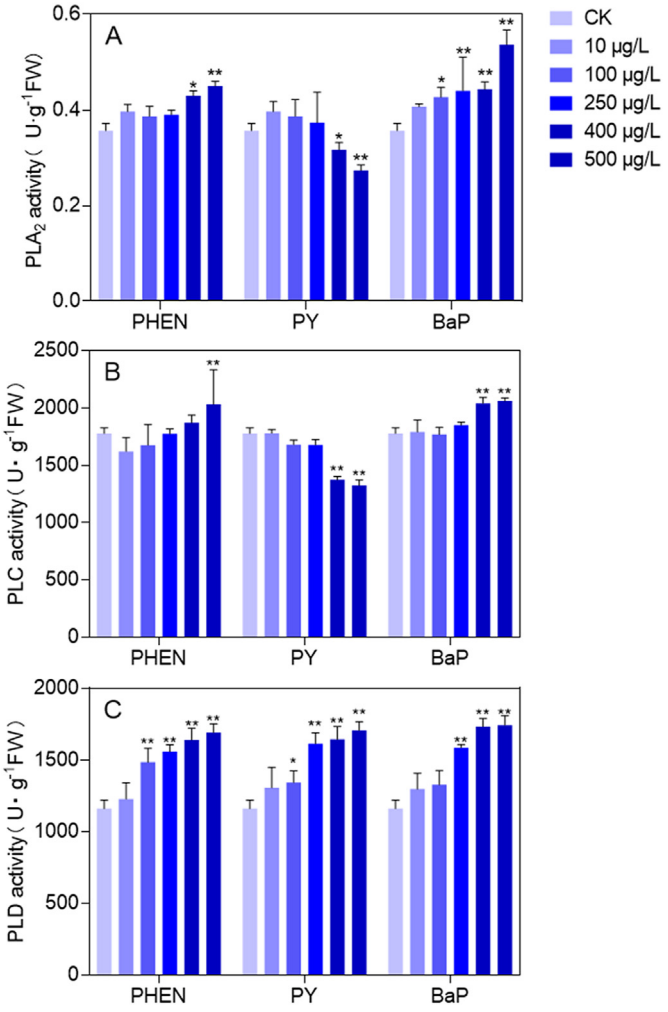

Fig. 5. PLA_2, PLC and PLD activity after being exposed to different concentrations of PHEN, PY and BaP. A: PLA_2 activity in shoots; B: PLC activity in shoots; C: PLD activity in shoots. *$p < 0.05$; **$p < 0.01$.

cell membranes, disruptions to membrane permeability, and initiation of programmed cell death processes (Babula et al., 2012; Sushkova et al., 2020b). The impacts on membrane integrity and permeability were likely due to the impaired PL synthesis, verified by the gene expression and targeted metabolic analyses below.

3.4. Activities of phospholipase and expressions of its encoding genes in response to PAHs

The synthesis of PLs was regulated by phospholipase, an enzyme that can hydrolyze PLs into fatty acids and other lipophilic substances during PL metabolism. Therein, phospholipase PLA_2, PLC, and PLD play critical roles in the synthesis and decomposition of PA, PG, and PE. In this study, the expressions of key genes encoding PLA_2, PLC, and PLD were determined in rice shoots after exposure to different concentrations of PHEN, PY, and BaP. The relative gene expression levels were largely consistent with the changes in enzymatic activities (Figs. 4 and 5).

The results showed that *PLA_2-3*, *PLA_2-4*, and *PLA_2-6* were firstly downregulated and then upregulated in shoots after being exposed to PHEN and BaP at all tested concentrations (Fig. 4). It has been shown that PLA_2 can be stimulated in response to biotic and abiotic stresses (Ryu, 2004). At an exposure level equal to or above 400 μg/L PHEN, the genes encoding PLA_2 were all upregulated, and the upregulation was as high as 2-fold at 500 μg/L. The PLA_2 activity increased by a maximum of 26.2% during the exposure to 500 μg/L PHEN. Similarly, with the exposure to BaP at 250 μg/L or above, all three genes were significantly upregulated, and the activity of PLA_2 also increased. These results are in agreement with the changes in targeted PLs. BaP at 500 μg/L strongly repressed the expressions of the three genes encoding PLA_2, whereas PY-induced repressions were observed at concentrations as low as 10 μg/L. Numerically, at 10–500 μg/L PY, *PLA_2-3*, *PLA_2-4*, and *PLA_2-6* were significantly downregulated 18.9–27.9%, 18.7–24.3%, and 19.4–26.3%, respectively. PLA_2 activity decreased by 23.4% at 500 μg/L PY. These results suggest that PY inhibit the expression of PLA_2-encoding genes and the activity of PLA_2 to much higher levels than PHEN and BaP.

PHEN ranged from 10 to 500 μg/L generally increased the expressions of *PLC-1*, *PLC-2*, and *PLC-4* to 0.76–4.1, 1.8–11.0, and 1.0–5.7 fold, respectively. The PLC activity increased by a maximum of 14.4% during the exposure to 500 μg/L PHEN. In contrast, these three genes were significantly downregulated (below 0.64-fold) upon exposure to BaP and then upregulated (above 3.0-fold at 500 μg/L). The activity of PLC transiently decreased and then increased, reaching a maximum of 116% of the controls at 500 μg/L BaP. Similar to changes in PLA_2-coding genes, *PLC-1*, *PLC-2*, and *PLC-4* were significantly downregulated 36.6–47.9%, 46.1–57.1%, and 71.9–175.0% after exposure to 10–500 μg/L PY. The maximum decrease in PLC activity was 25.6% at 500 μg/L PY (Fig. 5). The 4-, 5-, 9- and 10-position of PY are described as K-regions responsible for the carcinogenic effect of PY. The universal downregulation of PLA_2 and PLC encoding genes was probably due to the binding of PY's K-region to DNA (Pullman and Pullman, 1955). Meanwhile, *PLD-1*, *PLD-2*, and *PLD-4* were gradually upregulated in rice shoots with increasing exposure concentrations of PHEN, PY, and BaP. The PLD activity in rice shoots increased as the concentration of the three PAHs increased. BaP exposure induced the largest changes in PLD-encoding gene expression compared with PHEN and PY exposure. When exposed to 500 μg/L of BaP, *PLD-1* was upregulated by more than 5.0-fold. The activity of PLD increased by 50.3% at 500 μg/L BaP. Previous studies have shown that external stress induces activation of PLD leading to PL hydrolysis, with disturbance of the cell membrane integrity (Ryu and Wang, 1996).

A PL metabolic network was constructed based on known pathways in the endoplasmic reticulum (Fig. 6). DAG and PA are the important intermediates in PL homeostasis; they serve both as the

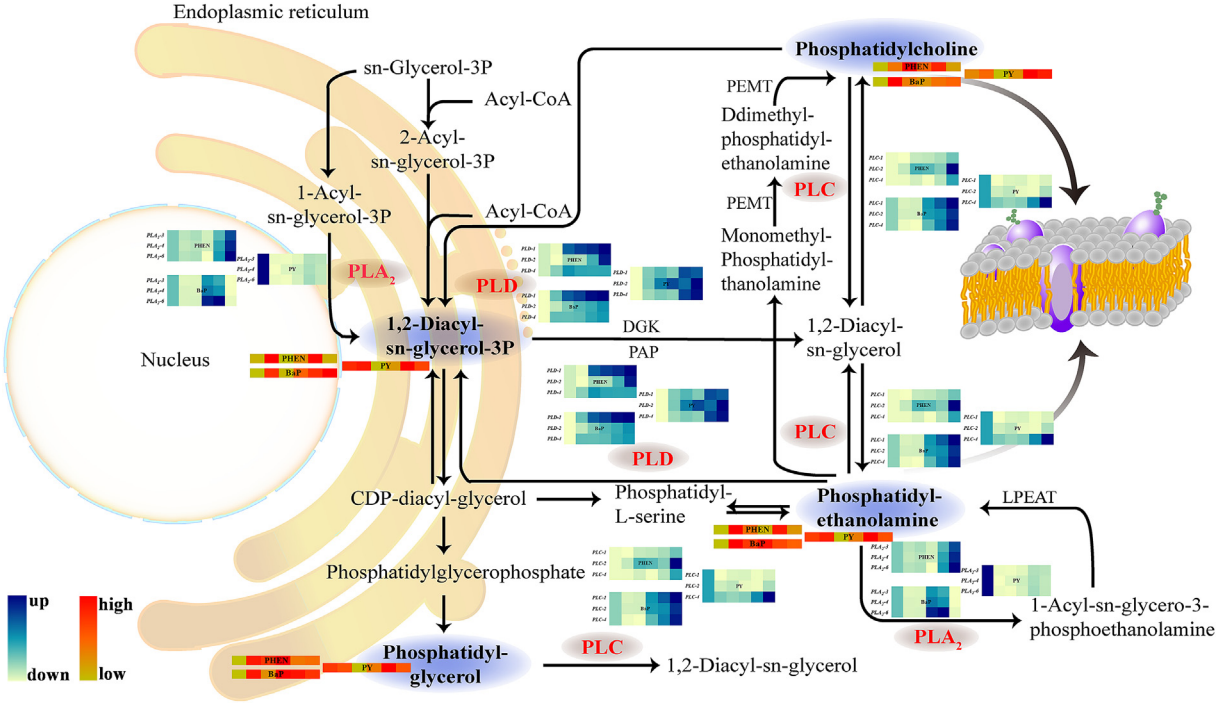

Fig. 6. A schematic of the phospholipid metabolic network in *Oryza sativa*. Changes in metabolites and gene expression levels mapped to phospholipid metabolism were shown in rice shoots at six exposure concentrations of PHEN, PY and BaP (0, 10, 100, 250, 400 and 500 μg/L). The relative content of each phospholipid metabolite in rice shoots was displayed in the form of a heat map from low (green) to high (red) as presented in the color scale. Enzymes involved in phospholipid metabolism pathway were marked in red and the genes encoding the enzymes were put beside them. Similarly, the gene expression levels were denoted in blue (up-regulated) and yellow (down-regulated). Six columns from left to right for each phospholipid metabolite and gene represented groups treated with 0, 10, 100, 250, 400 and 500 μg/L of PHEN, PY and BaP. (For interpretation of the references to color in this figure legend, the reader is referred to the Web version of this article.)

substrates of PL synthesis and the products of PL degradation. PLD and PLC are involved in the hydrolysis of the PLs PC and PE to PA and DAG (Gu et al., 2017). DAG was produced by phospholipase C, which catalysed the hydrolysis of PG to DAG. Lysophosphatidylethanolamine (LPE) was mainly generated from PLA_2-catalysed hydrolysis of PE. PLA_2 catalysed the conversion of 1-acyl-sn-glycerol-3-phosphate to 1, 2-diacyl-sn-glycerol-3-phosphate (Li-Beisson et al., 2010).

Varied abundances in PLs may reflect the impacts of PHEN, PY, and BaP on their synthesis and degradation. PHEN and BaP induced the upregulation of key genes encoding PLA_2, PLC, and PLD, and the enzymatic activities. The contents of PLs in shoots increased. The increased membrane PLs help maintain membrane stability and integrity (Lim et al., 2007). In line with the PY-induced downregulations of the PLA_2 and PLC encoding genes and the decreased enzyme activities, PA and DAG also significantly decreased. The loss of DAG as a precursor resulted in decreased PC and PE contents in shoots and the cell membrane. The decrease in PA further hampered the synthesis of PG via the CDP-DAG pathway. The extensive downregulation of PLs and their synthesis-related genes by PY supports the more severely damaged cell membranes.

4. Conclusion

The accumulation of organic pollutants in plants poses a severe threat to food safety. In this study, the multifaceted impacts of PY, PHEN, and BaP on rice roots and shoots were evaluated, including pollutant distributions, changes in biomass, cell membrane integrity, expression of key genes involved in PL synthesis, and the abundance of intracellular PLs. Among the three PAHs, PHEN accumulated to the highest level inside the crop due to its low logK_{ow}. However, PY induced the most severe cell membrane damage, inhibited the activities and encoding gene expression of phospholipase, and reduced the PLs contents. Exposure to 10–500 μg/L PY resulted in downregulation of the phospholipase A_2 genes *PLA_2-3, PLA_2-4,* and *PLA_2-6* (to 19% of the control without exposure) and phospholipase C genes *PLC-1*, *PLC-2,* and *PLC-4* (to 50% of the control), consistent with the changes in phospholipase activity. The contents of four typical PLs also decreased to a greater extent than those in the PHEN- and BaP-exposed groups. Future studies should focus on the transport mechanism of PY into cells, its metabolism within crop tissues, as well as the broader impacts on pathways related to growth and grain quality. More omics-based approaches and isotopic tracing could be applied to resolve the above issues. The results of this study would contribute to the global endeavors on preventing PAH pollution and reducing its adverse impacts on food safety and quality.

Author statement

Liu Shuang: Experiments, Data curation, Writing – original draft. Methodology, Software; **Liu Na**: Software, Investigation, Writing- Reviewing and Editing; **Lu Huijie**: Writing- Reviewing and Editing. **Zhu lizhong**: Supervision, Writing- Reviewing and Editing.

Declaration of competing interest

The authors declare that they have no known competing financial interests or personal relationships that could have appeared to influence the work reported in this paper.

Acknowledgments

This work was supported by the National Natural Science Foundation of China (21836003, 21906143 and 21621005).

Appendix A. Supplementary data

Supplementary data to this article can be found online at https://doi.org/10.1016/j.envpol.2021.117073.

References

Ahammed, G.J., Yuan, H.L., Ogweno, J.O., Zhou, Y.H., Xia, X.J., Mao, W.H., Kai, S., Yu, J.Q., 2012. Brassinosteroid alleviates phenanthrene and pyrene phytotoxicity by increasing detoxification activity and photosynthesis in tomato. Chemosphere 86, 546–555.
Alexander, Martin, 2000. Aging, bioavailability, and overestimation of risk from environmental pollutants. Environ. Sci. Technol. 34, 4259–4265.
Babula, P., Vodicka, O., Adam, V., Kummerova, M., Havel, L., Hosek, J., Provaznik, I., Skutkova, H., Beklova, M., Kizek, R., 2012. Effect of fluoranthene on plant cell model: tobacco BY-2 suspension culture. Environ. Exp. Bot. 78, 117–126.
Burken, J.G., Schnoor, J.L., 1997. Uptake and metabolism of atrazine by poplar trees. Environ. Sci. Technol. 31, 1399–1406.
Bustamant, C.A., Brotman, Y., Monti, L.L., Gabilondo, J., Budde, C.O., Lar, M.V., Fernie, A.R., Drincovich, M.F., 2017. Differential lipidome remodeling during postharvest of peach varieties with different susceptibility to chilling injury. Physiol. Plantarum 163, 2–17.
Cavallo, D., Ursini, C.L., Bavazzano, P., Cassinelli, C., Frattini, A., Perniconi, B., Francesco, A.D., Ciervo, A., Rondinone, B., Iavicoli, S., 2006. Sister chromatid exchange and oxidative DNA damage in paving workers exposed to PAHs. Ann. Occup. Hyg. 50, 211–218.
Chen, J., Le, X.C., Zhu, L.Z., 2019a. Metabolomics and transcriptomics reveal defense mechanism of rice (*Oryza sativa*) grains under stress of 2,2',4,4'-tetrabromodiphenyl ether. Environ. Int. 133, 105154.
Chen, M.S., Guo, H.M., Chen, S.Q., Li, T.T., Li, M.Q., Rashid, A., Jie, X.C., Wang, K., 2019b. Methyl jasmonate promotes phospholipid remodeling and jasmonic acid signaling to alleviate chilling injury in peach fruit. J. Agric. Food Chem. 67, 9958–9966.
Choi, S.K., Takahashi, E., Inatsu, O., Mano, Y., Ohnishi, M., 2005. Component fatty acids of acidic glycerophospholipids in rice grains: universal order of unsaturation index in each lipid among varieties. J. Oleo Sci. 54, 369–373.
Cowan, A.K., 2006. Phospholipids as plant growth regulators. Plant Growth Regul. 48, 97–109.
Craddock, C.P., Adams, N., Bryant, F.M., Kurup, S., Eastmond, P.J., 2015. Phosphatidic acid phosphohydrolase regulates phosphatidylcholine biosynthesis in arabidopsis by phosphatidic acid-mediated activation of ctp: phosphocholine cytidylyltransferase activity. Plant Cell 27, 1251–1264.
Downward, G.S., Hu, W., Rothman, N., Reiss, B., Wu, G.P., Wei, F., Chapman, R.S., Portengen, L., Qing, L., Vermeulen, R., 2014. Polycyclic aromatic hydrocarbon exposure in household air pollution from solid fuel combustion among the female population of xuanwei and fuyuan Counties, China. Environ. Sci. Technol. 48, 14632–14641.
Epa, U., 2016. Estimation Programs Interface Suite™ for Microsoft® Windows, V. 4.11 or Insert Version Used. United States Environmental Protection Agency, Washington, DC, USA.
Gu, Y.N., He, L., Zhao, C.J., Wang, F., Yan, B.W., Gao, Y.Q., Li, Z.T., Yang, K.J., Xu, J.Y., 2017. Biochemical and transcriptional regulation of membrane lipid metabolism in maize leaves under low temperature. Front. Plant Sci. 8, 2053.
Hoagland, D.R., Arnon, D.I., 1950. The water culture method for growing plants without soil. Circ. California Agric. Exp. Station 347, 305–311.
Hong, Y., Yuan, S., Sun, L., Wang, X., Hong, Y., 2018. Cytidinediphosphate-diacylglycerol synthase 5 is required for phospholipid homeostasis and is negatively involved in hyperosmotic stress tolerance. Plant J. 94, 1038–1050.
Huang, Y., Song, Y., Huang, J., Xi, Y., Johnson, D., Liu, H., 2019. Selenium alleviates phytotoxicity of phenanthrene and pyrene in *Alternanthera Philoxeroides*. Int. J. Phytoremediation 1–8.
Huo, X., Wu, S., Zhu, Z., Liu, F., Fu, Y., Cai, H., Sun, X., Gu, P., Xie, D., Tan, L., Sun, C., 2017. NOG1 increases grain production in rice. Nat. Commun. 8, 1497.
Kang, F.X., Chen, D.S., Gao, Y.Z., Zhang, Y., 2010. Distribution of polycyclic aromatic hydrocarbons in subcellular root tissues of ryegrass (*Lolium multiflorum* Lam.). BMC Plant Biol. 10, 210.
Karlowski, W.M., Heiko, S., Vijayalakshmi, J., Volker, S., Mayer, K.F.X., 2003. MOsDB: an integrated information resource for rice genomics. Nucleic Acids Res. 31, 190–192.
Kroon, J., 2011. Phosphatidic acid phosphohydrolase 1 and 2 regulate phospholipid synthesis at the endoplasmic reticulum in Arabidopsis. Plant Cell 22, 2796–2811.
Li-Beisson, Y., Shorrosh, B., Beisson, F., Andersson, M.X., Arondel, V., Bates, P.D., Baud, S., Bird, D., Debono, A., Durrett, T.P., 2010. Acyl-lipid metabolism. Arabidopsis Book 8, e0133.
Li, Z.H., Wang, W., Zhu, L.Z., 2020. A three-phase-successive partition-limited model to predict plant accumulation of organic contaminants from soils treated with surfactants. Environ. Pollut. 261, 114071.
Lim, P.O., Kim, H.J., Gil Nam, H., 2007. Leaf senescence. Annu. Rev. Plant Biol. 58, 115–136.

Lin, F., Sun, J., Liu, N., Zhu, L.Z., 2020. Phytotoxicity and metabolic responses induced by tetrachlorobiphenyl and its hydroxylated and methoxylated derivatives in rice (*Oryza sative* L.). Environ. Int. 139, 105695.
Liu, H., Weisman, D., Ye, Y.B., Cui, B., Wang, Z.H., 2009. An oxidative stress response to polycyclic aromatic hydrocarbon exposure is rapid and complex in *Arabidopsis thaliana*. Plant Sci. 176, 375–382.
Liu, L., Waters, D.L., Rose, T.J., Bao, J., King, G.J., 2013. Phospholipids in rice: significance in grain quality and health benefits: a review. Food Chem. 139, 1133–1145.
Livak, K.J., Schmittgen, T.D., 2002. Analysis of relative gene expression data using Real-Time Quantitative PCR. Method 25, 402–408.
Mao, L., Pang, H., Wang, G., Zhu, C., 2007. Phospholipase D and lipoxygenase activity of cucumber fruit in response to chilling stress. Postharvest Biol. Technol. 44, 42–47.
Pan, L.L., Sun, J.T., Le, X.C., Zhu, L.Z., 2018. Effect of copper on the translocation and transformation of polychlorinated biphenyls in rice. Chemosphere 193, 514–520.
Pretorius, T.R., Charest, C., Kimpe, L.E., Blais, J.M., Ma, Y., 2018. The accumulation of metals, PAHs and alkyl PAHs in the roots of *Echinacea purpurea*. PloS One 13, e0208325.
Pullman, A., Pullman, B., 1955. Electronic structure and carcinogenic activity of aromatic molecules: new developments. Adv. Canc. Res. 3, 117–169.
Rajput, V., Minkina, T., Semenkov, I., Klink, G., Sushkova, S., 2021. Phylogenetic analysis of hyperaccumulator plant species for heavy metals and polycyclic aromatic hydrocarbons. Environ. Geochem. Health 43, 1629–1654.
Ren, L., Huang, X.D., Mcconkey, B.J., Dixon, D.G., Greenberg, B.M., 1994. Photoinduced toxicity of three polycyclic aromatic hydrocarbons (fluoranthene, pyrene, and naphthalene) to the duckweed *Lemna gibba* L. G-3. Ecotoxicol. Environ. Saf. 28, 160–171.
Ryu, S.B., 2004. Phospholipid-derived signaling mediated by phospholipase A in plants. Trends Plant Sci. 9, 229–235.
Ryu, S.B., Wang, X., 1996. Activation of phospholipase D and the possible mechanism of activation in wound-induced lipid hydrolysis in castor bean leaves. Biochim. Biophys. Acta 1303, 243–250.
Sayyari, M., Babalar, M., Kalantari, S., Serrano, M., Valero, D., 2009. Effect of salicylic acid treatment on reducing chilling injury in stored pomegranates. Postharvest Biol. Technol. 53, 152–154.
Schinecker, T.M., Perlow, R.A., Suse, B., Geacintov, N.E., Sci Cc Hitano, D.A., 2003. Human RNA polymerase II is partially blocked by DNA adducts derived from tumorigenic benzo[c]phenanthrene diol epoxides: relating biological consequences to conformational preferences. Nucleic Acids Res. 6004–6015.
Sun, J., Liu, J., Miao, Y., Chang, W., Sun, Y., Zhang, A., Wang, T., Zhen, L., Jiang, G., 2013. In vivo metabolism of 2,2',4,4'-tetrabromodiphenyl ether (BDE-47) in young whole pumpkin plant. Environ. Sci. Technol. 47, 3701–3707.
Sushkova, S.N., Minkina, T., Tarigholizadeh, S., Antonenko, E., Kizilkaya, R., 2020a. PAHs accumulation in soil-plant system of *Phragmites australis* Cav. in soil under long-term chemical contamination. Euras. J. Soil Sci. 9, 242–253.
Sushkova, S.N., Minkina, T., Tarigholizadeh, S., Rajput, V.D., Batukaev, A., 2020b. Soil PAHs Contamination Effect on the Cellular and Subcellular Organelle Changes of Phragmites Australis Cav. Environmental Geochemistry and Health.
Sverdrup, L.E., Krogh, P.H., Nielsen, T., Kjaer, C., Stenersen, J., 2003. Toxicity of eight polycyclic aromatic compounds to red clover (*Trifolium pratense*), ryegrass (*Lolium perenne*), and mustard (*Sinapsis alba*). Chemosphere 53, 993–1003.
Tang, D., Kryvenko, O.N., Wang, Y., Jankowski, M., Trudeau, S., Rundle, A., Rybicki, B.A., 2013. Elevated polycyclic aromatic hydrocarbon-DNA adducts in benign prostate and risk of prostate cancer in African Americans. Carcinogenesis 34, 113–120.
Tong, C., Lei, L., Waters, D., Bao, J.S., 2016. Association mapping and marker development of genes for starch lysophospholipid synthesis in rice. Rice Sci. 23, 287–296.
Vaz Pedroso, A.N., Bussotti, F., Papini, A., Tani, C., Domingos, M., 2016. Pollution emissions from a petrochemical complex and other environmental stressors induce structural and ultrastructural damage in leaves of a biosensor tree species from the Atlantic Rain Forest. Ecol. Indicat. 67, 215–226.
Wu, X., Wang, W., Zhu, L.Z., 2018. Enhanced organic contaminants accumulation in crops: mechanisms, interactions with engineered nanomaterials in soil. Environ. Pollut. 240, 51–59.
Wu, X., Zhu, L.Z., 2019. Prediction of organic contaminant uptake by plants: modified partition-limited model based on a sequential ultrasonic extraction procedure. Environ. Pollut. 246, 124–130.
Zhao, Y.Y., Qian, C.L., Chen, J.C., Peng, Y., Mao, L.C., 2010. Responses of phospholipase D and lipoxygenase to mechanical wounding in postharvest cucumber fruits. J. Zhejiang Univ. (Humanit. Soc. Sci.) B 443–450.
Zhu, Y., Wang, K., Wu, C., Zhao, Y., Xu, C., 2019. Effect of ethylene on cell wall and lipid metabolism during alleviation of postharvest chilling Injury in peach. Cells 8, 1612.